EVALUATING THE DYNAMIC BEHAVIOUR OF CONCRETE SLAB TRACK FOR HIGH SPEED RAIL USING NUMERICAL ANALYSIS

Railway Engineering-2017 railwayengineering.com doi: 10.25084/raileng.2017.0131

EVALUATING THE DYNAMIC BEHAVIOUR OF CONCRETE SLAB TRACK FOR HIGH SPEED RAIL USING NUMERICAL ANALYSIS

L Zimele, R De Bold & M C Forde
University of Edinburgh
School of Engineering
The Kings Buildings
Edinburgh EH10 6BN
UK

C L Ho
University of Massachusetts, Amherst
Dept of Civil & Environmental Engineering
28 Marston Hall, 130 Natural Resources Road
Amherst, MA 01003
USA

KEYWORDS: High Speed, Railway, Dynamic Behaviour, Numerical Analysis

ABSTRACT

Substantial investments in high-speed railway lines have led to an increase in train speeds. A major problem of this is the generation of excessive ground vibrations, predominantly caused by surface or Rayleigh waves, which contribute to approximately two thirds of the total wave energy. Yet there is no simplistic modelling data presentation available. This work therefore aims to find a relationship between normalised maximum dynamic displacement (with respect to maximum static displacement) and normalised train speed (with respect to the Rayleigh wave velocity) for both ballasted and slab tracks.

2-D models of the problem were constructed using the finite element method and Abaqus software. Static and dynamic analyses were then performed on different track configurations and a range of subsoil parameters. The variation of maximum dynamic displacements further afield was explored for 15 train speeds, and the results compared with the experimental field data from three European train lines: Ledsgaard (Sweden), Amsterdam-Utrecht (The Netherlands) and Stilton Fen (UK).

The modelling results slightly overestimated the maximum dynamic displacement values; hence, mean calibration factors and additional, more precise material properties were proposed to fit the field data. It was concluded that the slab track does not amplify the maximum dynamic displacements to the same extent as the ballasted track. It was found that substituting the ballasted track on an embankment with concrete slab track would reduce the maximum dynamic displacement at the maximum allowable train speed (typically 0.7 x Rayleigh wave velocity) by approximately 30%.

INTRODUCTION

A major problem with elevated train speeds is an increase in ground vibrations (Connolly et al, 2015). This could subsequently lead to a degraded ballasted structure and even derailment in an extreme case, creating danger to travelling passengers. Additionally, increased vertical ground deflections, the majority of which travel in the form of Rayleigh waves further afield, could cause excessive vibrations, noise and damage in the surrounding structures.

Very little of the current research in this field has been carried out on concrete slab tracks. This research aims to compare the performance of trains running on both concrete slab track and ballasted track. Additionally, different soil parameters and track configurations are explored, including a track on a flat surface and an embankment. The main output investigated is time-dependent vertical displacements at discrete points outwards from the track, which are acquired from the history output data in Abaqus CAE.

HIGH-SPEED RAIL GENERATED GROUND VIBRATIONS

The two main mechanisms that generate ground-borne vibrations are quasi-static and dynamic load excitations from passing trains. Both mechanisms have been well documented in the work by Lombaert and Degrande (2009). The former is related to the static axle loads, which are time dependent and vary periodically when the train is moving. The loading can be considered quasi-static only at low frequencies, defined up to 50Hz. Downwards track deflections are dominant in the case of quasi-static loading.

Dynamic load excitation, however, considers the dynamic effects caused by a moving train at higher frequencies (above 50Hz). The main sources of the behavioural change of the loading type are imperfections of the rail or wheel and heterogeneities in rail connections, which lead to a variation of rail stiffness along its length. The unevenness of the rail can be expressed as a power spectral density function (PSD), and the dynamic loading as a stationary random process. Vibrations in the field outward from the track dominate in the case of dynamic load excitation.

As 2-D models perpendicular to the longitudinal track direction are the main focus of this research, all loading scenarios will initially be analysed as quasi-static. In fact, quasi-static wheel-axle pressure is the most common load excitation, as it is present even for ideally flat rails and wheels (Krylov, V. V., et al., 2000).

WAVE PROPAGATION FROM HIGH-SPEED RAIL

There are two main categories of waves that propagate in the track and travel further in the field: body and surface waves. Pressure and shear waves are defined as body waves, and travel under the surface of the subsoil layer. Pressure waves travel in longitudinal direction, while shear waves travel in transverse direction. Surface waves are Rayleigh waves that travel in an elliptical manner at the surface of the subsoil layer and decay with depth.

For this research, given that Rayleigh waves contribute to approximately 67% of the total wave energy, only Rayleigh wave velocity is considered (Connolly et al, 2015). In fact, it has been proven from detailed field measurements that the dynamic response of the track system depends on the first phase velocity of the Rayleigh mode of the underlying embankment and subsoil on site (in addition to the characteristic wavelengths of the site, and the spacing between the axles and bogies of the train (Madshus & Kaynia, 1999)).

PROBLEMS CAUSED BY EXCESSIVE VIBRATIONS

The data acquired from a high-speed train line running on soft soil in Sweden shows dynamic amplifications in the track/ embankment/ ground system as the train reaches some “critical velocity” (Kaynia & Madshus, 2000; Madshus & Kaynia, 1999). A “ground vibration boom” has also been previously described in literature (Krylov, 1995; Connolly & Forde, 2015). This phenomenon is associated with substantial amplification in vertical displacements due to resonance-like behaviour when the train has reached Rayleigh wave velocity. It was first demonstrated in Ledsgard, Sweden, where physical vibrations were felt by people, as well as large bending amplitudes of the masts carrying electric wires and premature depreciation of the rails were observed (Krylov, 2000).

There are two main critical velocities in the track-ground system to be considered: Rayleigh wave velocity in the surrounding subsoil medium and the track critical velocity. Based on the analytical models, the track critical velocity is predicted to be 10-30 % higher than the Rayleigh wave velocity for the same ground conditions (Krylov et al, 2000). The research is focused on the displacement behaviour

outwards from the track, with elevated train speeds tied to the Rayleigh wave velocity. It has been suggested that the train critical velocity can be restricted to 0.7 x Rayleigh wave velocity (Connolly & Forde, 2015). However, critical velocities can be as low as 160 – 180 km/h on soft soils (Krylov, 2000). This is a common problem; hence, it is of high importance to predict the behaviour of train-induced vibrations.

EXPERIMENTAL FIELD DATA

The experimental field data from three railway lines in Europe have been replicated (Connolly et al, 2014) in Figure 1. It shows the variation of maximum dynamic displacement normalised to the maximum static displacement with train velocity normalised to the subsoil Rayleigh wave velocity. It can be observed that maximum vertical displacements start to increase exponentially as the train speed reaches half the Rayleigh wave velocity in subsoil for a ballasted track (marked blue). Concrete slab track behaviour with increasing train speeds, relative to that of the ballasted track, was predicted as part of the initial stages of the project in the same Figure 1. The starting point at static state corresponds to the results acquired during another research project (Kece & Reikalas, 2016). It was shown that the load transfer from rail to slab is relatively half of that from the rail to the ballast layer.

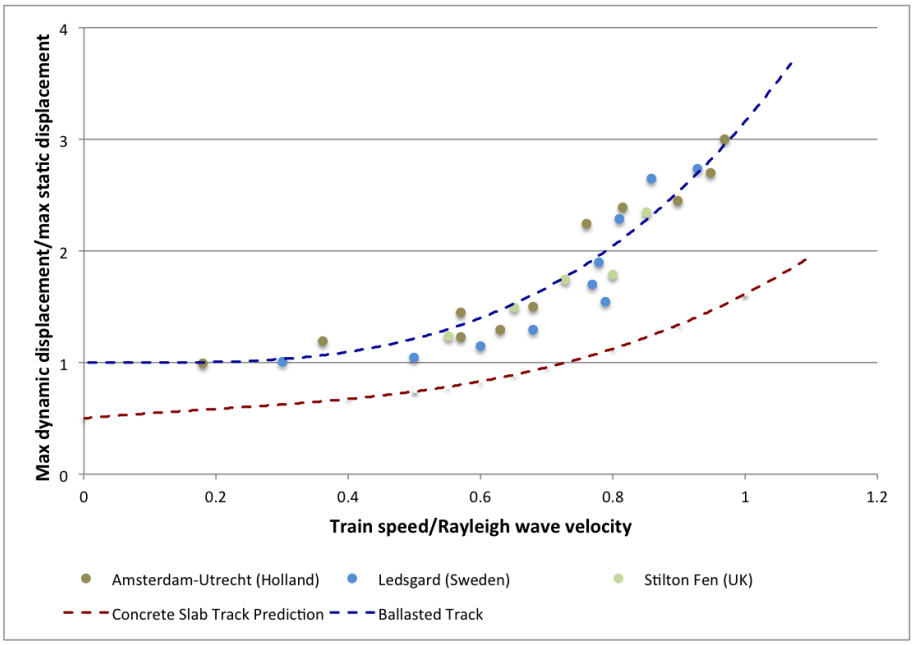

Figure 1 Normalised max dynamic displacement versus normalised train speed (replicated from Connolly, 2013)*

*The concrete slab track prediction is normalised to the ballasted track max static displacement, not its own max static displacement, thus originating at 0.5 on the y-axis rather than 1.

MODELLING OF TRACK AND GROUND VIBRATIONS

Previous Research

Modelling of track and ground vibrations has been a focus for research for the past few decades. With increased train speeds, there is a natural urge to estimate subsequent effects on the environment (Krylov, 1995). Earlier methods to model ground-borne vibrations were primarily analytical (Krylov, 1995; Dieterman and Metrikine, 1997; Krylov, et al., 2000; Kaynia, et al., 2000; Degrande and Lombaert, 2001; Paolucci, et al., 2003; Sheng, et al., 2004). Current methods focus commonly on numerical modelling

using the finite element method (FEM), which allows modelling of any track configuration, even ones with irregular geometry. The main disadvantage of this method is that when performed in three dimensions, it becomes computationally expensive. Generally, reducing the scope of the problem to two dimensions may overcome this problem.

2-dimensional modelling

Hall (2003) used axisymmetric models, perpendicular to the longitudinal direction, for observations of the vibration propagation outwards from the track, whils 2-D longitudinal models showed the vibration propagation within the track itself. For trains travelling below the Rayleigh wave velocity, it was shown that the wave fronts of the vibration propagation were perpendicular to the loads, while for the trains at higher than the Rayleigh wave velocity the wave fronts of the vibration propagation showed a plough-shaped behaviour following the loads. The difference between the relatively large calculated and measured shear strains was overcome by reducing the shear modulus of the subsoil.

Powrie, et al. (2007) investigated the stress changes under the ballasted track for dynamic loading, developing both 2-D and 3-D models. Both agreed well when the scaling of Young's modulus in 2-D was applied to account for the load distribution in the longitudinal direction.

Yang, et al. (2009) developed 2-D finite element models to analyse the stress path during the passage of a train. Different train speeds, acceleration/breaking scenarios and rail surface shapes were investigated. It was shown that as soon as the train speed reaches 10% of the Rayleigh wave velocity, significant dynamic effects influence the stress state of the soil. At the train speed of 50% of the Rayleigh wave velocity the shear stresses might be underestimated by as much as 30% in the static analysis. When the train is travelling at trans-Rayleigh speed, a vast increase in displacements and stresses is observed; the soil might fail. However, in the acceleration/braking areas, significant horizontal stresses are present, suggesting that soil might fail under shear failure criterion.

Another recent study, using 2-D numerical modelling (Kece and Reikalas, 2016), found that displacement peaks at points could be related to critical velocities and subsoil stiffness. It was also shown that peak displacement increased with speed. A parametric study of subsoil stiffness showed a possible 41% reduction in maximum RMS displacement. The developed 2-D models of both ballasted and concrete slab tracks showed 47% reduction in maximum RMS displacement for different train speeds. However, the results can be related to a train in static state only.

3-dimensional modelling

Zhai, et al. (2010) modelled an integrated train-track-subsoil system. The findings indicate there is a significant influence on the wheel/rail dynamic interaction caused by track irregularities. The vertical vibrations are also larger than the horizontal ones.

Kouroussis, G., et. al. (2011) modelled wheel-track interaction. Forces from that were applied to the soil subsystem, the interaction of which was provided by Winkler foundation, and was already included in the soil's stiffness. Both simulations were performed in the time domain to account for any non-linearities. This allowed for resolving the dynamic effects of the moving train.

Connolly (2013) studied the effect of changing embankment stiffness on the ground vibrations induced for a ballasted track with a constant train speed equal to 300 km/h, using a fully coupled 3-D model for the analyses. In addition, a new empirical prediction model was developed to account for soil properties

that could predict a variety of international vibration matrices; increased prediction performance was shown. Reduced vibrations were shown for stiffer embankments.

Huang and Chrismer (2013) developed a 3-D soil substructure model and combined it with Discrete Element Modelling (DEM) approach to investigate ballast settlements. It was concluded that increased train speeds cause amplification in track vibrations.

Ferreira and Lopez-Pita (2015) developed a complex 3-D model to predict ground-borne vibrations from high-speed trains. The method split the longitudinal direction of the track into several cross-sectional slices and reassembled them after processing allowing low computational time.

In general, an improvement for 2-dimensional models can be reached when adding an invariant third dimension in the longitudinal direction. This is done by using the 2.5-D modelling approach, which is less computationally expensive that the 3-D modelling approach, however it is not as effective.

Problem Statement

After reviewing available literature on the topic, it was concluded that a significant amount of work has been done to evaluate the dynamic behaviour of a ballasted track. Less work has been done for a concrete slab track. Moreover, a few problem areas for further research were identified.

It was noted that previously no explicit maximum displacement - train speed relationship has been numerically developed that would show information about train critical velocity and the corresponding dynamic displacements in a visually simple way (Connolly & Forde, 2015). Additionally, no experimental data of vertical vibrations are available for concrete slab tracks.

Furthermore, even though a 3-D model can account for longitudinal effects of the problem, overcoming a plane strain assumption, it is computationally expensive and very time consuming. However, 2-D models developed as part of another research project (Kece & Reikalas, 2016) are tied to a particular track design that cannot be disclosed (for commercial IPR reasons).

Consequently, it is of interest to be able to effectively predict the dynamic behaviour of a concrete slab track under elevated train speeds.

METHOD OF WORK

Abaqus CAE (graphical user interface) is used to both construct the different track types and to perform general static and dynamic, implicit analysis.

The track geometry was defined in two dimensions, as it was the purpose to test the ability of 2-D models to predict the dynamic effects. Four–node plane strain elements were used. The output of the software provided the vertical displacement values.

Three soil stiffnesses were initially chosen for a flat surface configuration (20MPa, 60MPa and 100 MPa). For an embankment configuration, additional subsoil stiffness of 600MPa were investigated to increase the Rayleigh wave velocity in the subsoil. This is to observe displacements at a distance from the track, by considering three data points.

ASSUMPTIONS

Plane strain elements were used for the analysis given that the system was very long, had identical cross-section, and the loading was equal in the longitudinal direction. These simplifications allowed for the problem to be treated in 2-D. However, this was a significant limitation, as in reality a track is not invariant in the longitudinal direction (rail unevenness, connections etc.).

It is correct to assume that whenever the subsoil stiffness is equal or greater to 120 MPa, no differential settlements can occur. Where secondary settlements are expected however, about 1.5% of reinforcement for B35 concrete and limited soil improvements are necessary (Esveld, 2003). The soil was assumed not to exceed the elastic limit strains, hence, it allowed the soil media to be analysed in the linear-elastic range.

"Rayleigh damping" is the most common form of damping in soils, and is expressed in terms of alpha damping ratio, α, which is proportional to mass, and beta damping ratio, β, which is proportional to stiffness.

Tie constraints with a surface-to-surface constraint type were used to model most interactions between the parts instances in the model assembly. This means that no relative movement between the surfaces was allowed.

Standard contact with particular transverse interaction and slip (no slip allowed) properties was defined for the four vertical surface contacts in each model: frost protection layer interaction with either subsoil directly or embankment for the slab track and sleeper interaction with the ballast layer for the ballasted track.

For the base and both sides of the subsoil layer, movement in vertical and horizontal directions and node rotation were prevented to ensure model stability. Encastre support conditions were used. This assumes a bedrock layer underlying the subsoil layer (Hall, 2003), which is not affected by any loading scenarios applied on top of the track, as the scope of the project focusses on the surface deformations.

The soil extends infinitely outwards from the track. However, it is impossible to model infinitely long elements in the finite element Abaqus software. This is overcome by introducing "infinite element layer" to both sides of the model. It serves as an absorbent for the vibrations. If not included, the vibrations would reflect backwards from the edge of the subsoil layer and contaminate the data.

Two alternative methods for modelling this in Abaqus exist: -

a) Manually alter the input file, changing the element type CPE4R to CINPE4;
b) Extend the subsoil layer and add extra layers on both sides with the same element size and main properties but significantly increased damping.

The second method allows for a simpler computation that can be easily applicable to all the required modelling situations, without compromising the accuracy of the results. This method was therefore applied in the models.

The loads for the dynamic analysis were inputted as tabular amplitude data. Figure 2 shows the points where the load is applied.

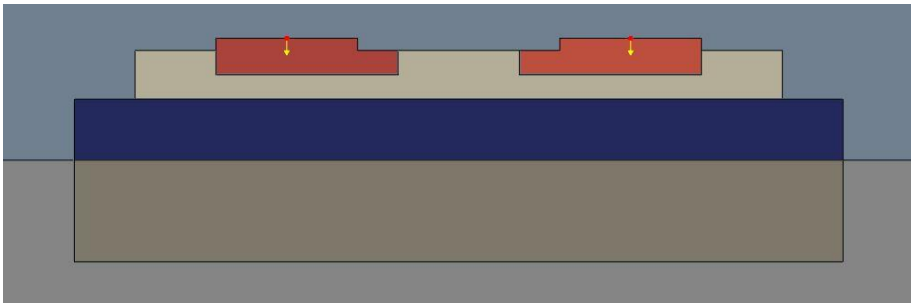

Figure 2 Points where the load is applied for the slab track model

Time dependent vertical displacements were requested for the field and history output data. To simplify the analysis, constant distances from the track/ embankment were considered. They are summarised in Table 1, and Figure 3 for embankment track configuration and Figure 4 for flat surface track configuration. Points were chosen with two main considerations in mind:

1. They must be further from the track not to be directly affected by the interactions between the physical parts of the model;
2. The spacing must be such as to allow the attenuation of the vibrations to be observed.

Table 1 Points considered in the analysis for all track configurations

Point	Distance from the Track/ Embankment, m
A	10
B	20
C	30

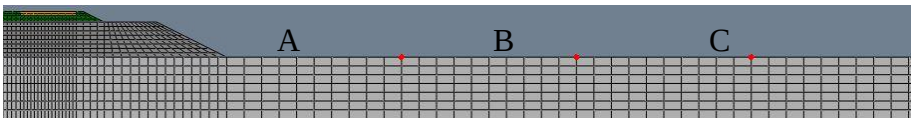

Figure 3 Points considered in the analysis for the embankment track configuration.

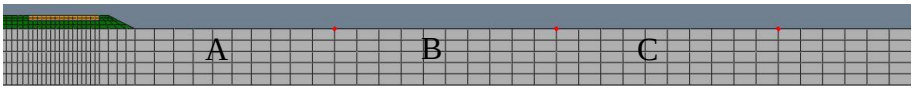

Figure 4 Points considered in the analysis for the flat surface configuration

LOADING SCENARIOS

A train wheel-to-rail loading signature, acquired from the empirical measurements from an Amtrak Acela train in Pennsylvania, USA, was used as the reference loading scenario. It was determined that the data is for a train travelling at 190km/h. Dynamic loading can be related to static loading using Eq 1 (AREMA).

$$P_v = P(1+\theta) \qquad \textbf{Eq 1}$$

P_v = vertical dynamic load
P = static load
θ is calculated from Eq 2 (AREMA)

$$\theta = \frac{d_{33}v}{100d_w} \qquad \text{Eq 2}$$

d_w = wheel diameter (inches)
d_{33} = wheel diameter of 33 inches
v = train speed (mph)

The wheel diameter was assumed to be $d_w = d_{33}$. A table of the static-to-dynamic loading factors, as per Eq 1 and Eq 2, can be seen in Table 2.

Table 2 Static-to-dynamic load factors for different train velocities

Train Speed, km/h	0	50	100	150	190	250	300	400	500
Factor	1	1.31	1.62	1.94	2.18	2.55	2.86	3.47	4.12

Furthermore, the nature of 2-dimensional modelling cannot account for the longitudinal stiffness of the rail, as the model is representing a cross-section of the track. This requires a load reduction factor to account for rail-to-ballast loading. As per previous research, this was determined to be 0.5 for rail-to-ballast (Kece & Reikalas, 2016). GeoTrack software, developed at the University of Massachusetts, suggests an approximate factor of 0.25 for the rail-to-slab. This is used for both static and dynamic load scaling. Consequently, the maximum static load for the Acela train derived from its 120.3kN peak load whilst travelling at 190kph is shown in Table 3 for slab and ballasted track.

Table 3 Maximum static load for different track types.

Track Type	Max. Static Load, kN
Slab	-13.796
Ballast	-27.592

The maximum static load values and the static-to-dynamic load factors can be used to produce loading signatures for different train speeds. Obviously, proportional scaling in the time domain would also need to be incorporated to account for the change in speed. An example of three different wheel-to-rail loading signatures can be seen in Figure 5 (the loading values would need to be factored by a further 0.5 or 0.25 to determine the actual rail-to-ballast or rail-to-slab loading values).

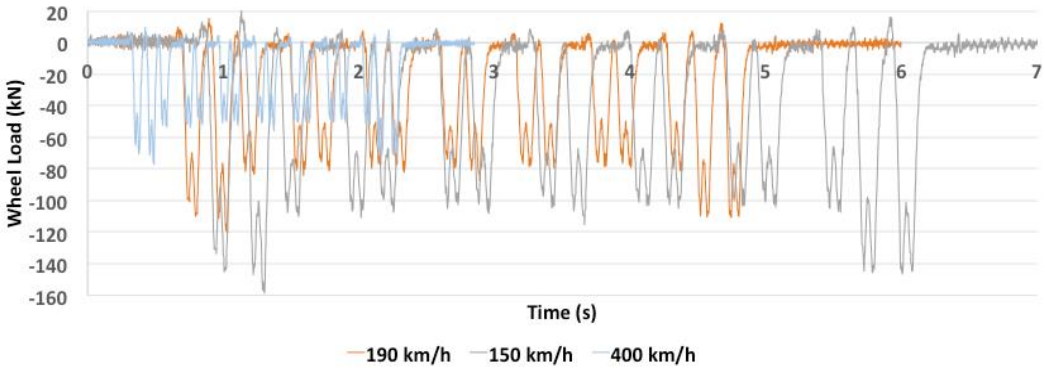

Figure 5 Wheel-to-rail loading signatures for train speeds of 150km/h, 190km/h, and 400km/h

MODEL DIMENSIONS

The Rheda 2000 track that was chosen for the slab track configuration, as it has been widely used in the railway industry (Rail One). Each track consists of a frost protection layer (FPL) embedded in the subsoil, a hydraulically bonded layer (HBL), a concrete bed, and two sleepers.

Figure 6 shows the subsoil model configuration used for all the models. Figure 7 shows dimensions of the slab track model configuration. Figure 8 shows the ballasted track dimensions. Figure 9 shows the slab track embankment dimensions. Figure 10 shows the ballasted track embankment dimensions. Figure 11 shows the mesh of the slab track on an embankment. Figure 12 shows the mesh of the ballasted track on an embankment.

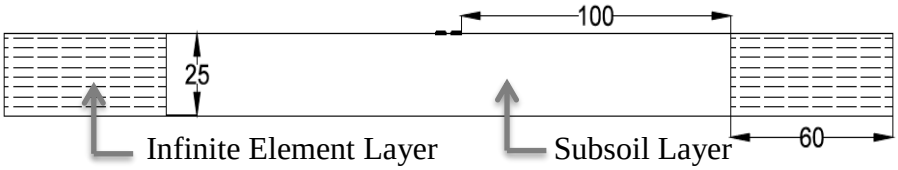

Figure 6 Subsoil space dimensions (in m) for models

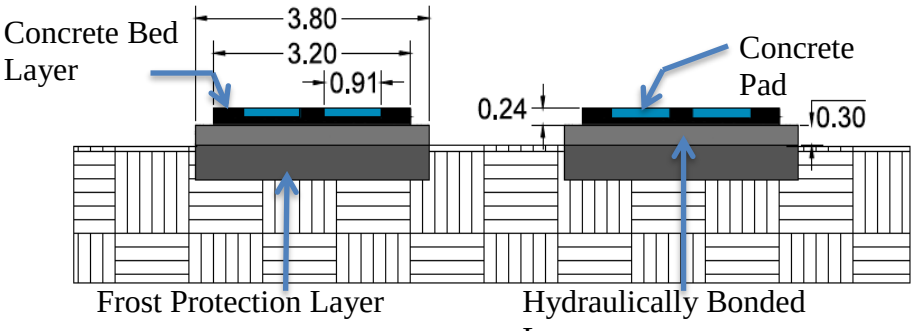

Figure 7 Slab track dimensions

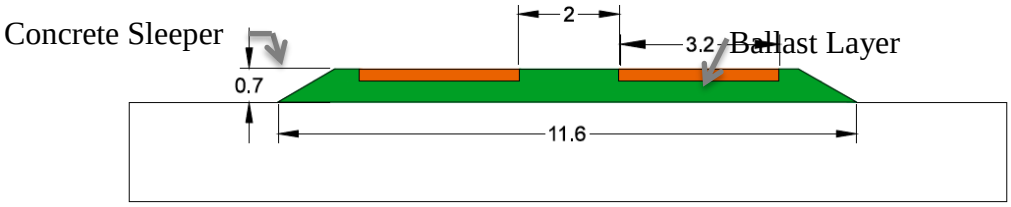

Figure 8 Ballasted track dimensions

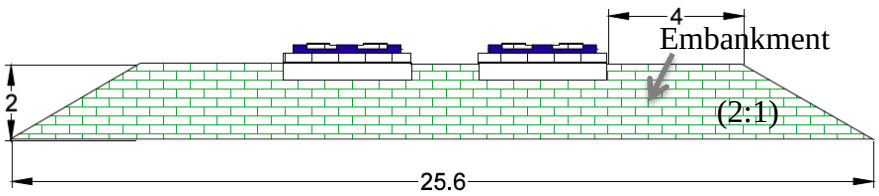

Figure 9 Slab track embankment dimensions

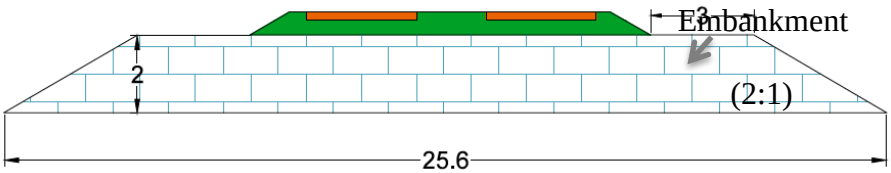

Figure 10 Ballasted track embankment dimensions

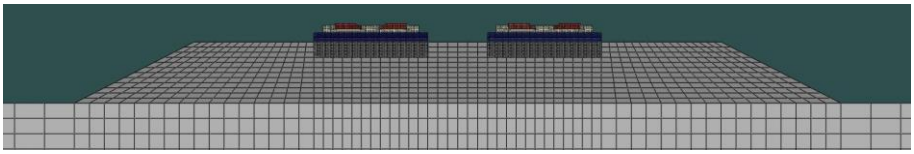

Figure 11 Mesh of the slab track on an embankment

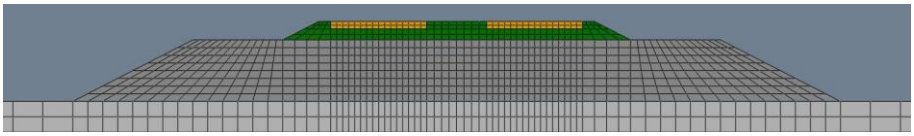

Figure 12 Mesh of the ballasted track on an embankment.

MODEL PARAMETERS

Table 4 summarises the commonly used material properties for the physical parts in the final model assembly, while Table 5 shows the subsoil stiffness values investigated for each track type, as well as the embankment properties (medium stiff). Subsoil of 600 MPa is not included for the models on a flat surface configuration, as the speeds of trains travelling on such configuration tracks will not fall in the high-speed range.

Table 4 Material properties for the track sections in the final model

Track Type	Section	Young's Modulus, E (MPa)	Density, ρ (kg/m^3)	Poisson's Ratio, ν (-)
Slab	Sleeper	32,000	2500	0.25
	Concrete Bed	30,000	2400	0.30
	HBL	200	1800	0.40
	FPL	100	1800	0.40
Ballast	Sleeper	32,000	2500	0.25
	Ballast	300	1800	0.35

Table 5 Subsoil and embankment stiffness in the final model

Track Configuration	Section	Young's Modulus, E (Mpa)	Density, ρ (kg/m^3)	Poisson's Ratio, ν (-)
Flat Surface	Subsoil	20, 60, 100	1800	0.49
Embankment	Subsoil	20, 60, 100, 600	1800	0.49
	Embankment	330	1725	0.29

The damping was calculated in accordance with Hashash and Park (2004), using Eq 3 and Eq 4.

$$\begin{bmatrix}\xi_m \\ \xi_n\end{bmatrix} = \frac{1}{4\pi}\begin{bmatrix}\frac{1}{f_m} & f_m \\ \frac{1}{f_n} & f_n\end{bmatrix}\begin{bmatrix}\alpha \\ \beta\end{bmatrix}$$

n = mode number
f = natural frequency of mode
α = mass proportional damping
β = stiffness proportional damping

Eq 3

$$f = \frac{v_s}{4H}(2n-1)$$

v_s = shear wave velocity
H = height of the soil column
ξ_m, ξ_n = effective damping ratio (ratio of actual to critical damping)

Eq 4

Mode numbers represent the first and highest natural frequencies of the undamped system. Hence, from the initial mode: n = 1 (for f_m) and n = 2 (for f_n). The effective damping is usually in the range of 1-5% (Hashash and Park, 2004). At 5% effective damping applied to the model, no wave propagation was observed; hence, 1% damping was chosen to proceed. Table 6 summarises the α and β values for different subsoil stiffness values.

Table 6 Damping ratios for different subsoil stiffness values

Subsoil Stiffness, Mpa	α	β
20	0.0580	0.0520
60	0.0996	0.0240
100	0.1280	0.0297
600	0.3150	0.0094

Every 1000th value from the loading scenarios is used in the analyses as shown in Figure 13. Even though several peaks are disregarded this way, the loading pattern still generally resembles that of the original loading data available (representing the critical aspects of the loading).

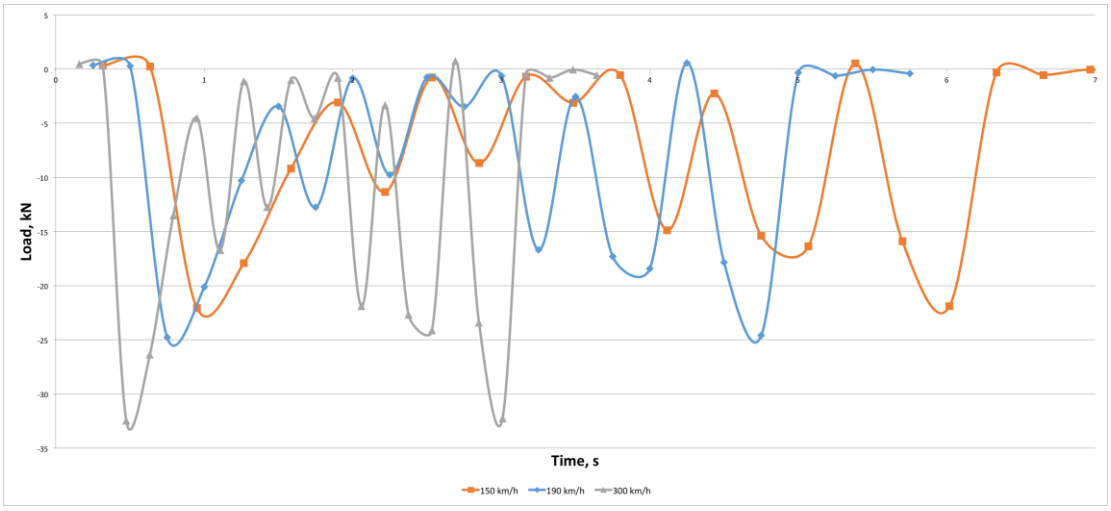

Figure 13 Combined load scaling for trains travelling at 150km/h, 190km/h, 300km/h

RESULTS SAMPLING

Loading periods corresponding to each train speed were determined from the original loading data available. As the loading was linearly scaled in the time domain, the sampling frequency of the output data points linearly increases with elevated train speeds. At least 4 sampling output data points in one loading period were advised for the sampling frequency. It was decided to sample at 0.125 of the loading period. Thus, 8 output data points are acquired during one loading period. Table 7 summarises the sampling frequency for different train velocities.

Table 7 Output data sampling frequencies for various train velocities

Train Velocity, km/h	Sampling Frequency, s
50	0.082
100	0.043
150	0.029
190	0.023
250	0.017
300	0.014
400	0.011
500	0.008

RAYLEIGH WAVE VELOCITY

Rayleigh wave velocity is a highly important parameter in the final presentation of the results, as this is the value to which different train speeds are normalised. Two approaches can be used to determine the Rayleigh wave velocity. It can be theoretically predicted using material properties: Young's modulus, E, density, ρ, and Poisson's ratio, ν. It can also be determined by observing the time of arrival of the first wave peak at different distances from the track.

Theoretical values for Rayleigh wave velocity can be derived from the following subsoil input parameters: Young's modulus, E, density, ρ, and Poisson's ratio, ν. Four soils of different parameters are investigated throughout the project, as summarised in Table 8.

Table 8 Subsoil parameters used in modelling

	Young's Modulus, E (Mpa)	Density, ρ (kg/m^3)	Poisson's Ratio, ν (-)
Subsoil 1	20	1800	0.49
Subsoil 2	60	1800	0.49
Subsoil 3	100	1800	0.49
Subsoil 4	600	1800	0.49

The following calculations are in accordance with Rahman and Michelitsch (2006). The shear wave velocity is found using Eq 5. The relationship for Rayleigh wave velocity, v_R, is then given in Eq 6, where K is correlation factor, expressed from Eq 7.

$$v_s = \sqrt{\frac{G}{\rho}}$$

v_s = shear wave velocity
ρ = density
G = shear modulus

Eq 5

$$K = \frac{v_R}{v_S}$$

v_R = Rayleigh wave velocity

Eq 6

$$K = \frac{0.87 + 1.12\nu}{1 + \nu}$$

K = correlation factor

Eq 7

Table 9 summarises the theoretical Rayleigh wave velocities for the four different soils investigated.

Table 9 Theoretically predicted Rayleigh wave velocity values

	Subsoil 1	Subsoil 2	Subsoil 3	Subsoil 4
Shear Wave Velocity, v_s (km/h)	220	382	492	1204
K	0.95	0.95	0.95	0.95
Rayleigh Wave Velocity, v_R (km/h)	209	364	468	1144

Experimental Rayleigh wave velocity values can be acquired from the time-dependent vertical displacement plots for points at varying distance from the track. The chosen points are shown in Figure 14, and their respective vertical displacements are shown in Figure 15. Distances from track to the points are recorded in

Table 10 (distances differ slightly for the different track types due to meshing requirements in each case). Only flat surface track configuration is considered, as it will be shown that the Rayleigh wave velocity depends on the subsoil material parameters only.

Figure 14 Points considered for determination of the Rayleigh wave velocity

Table 10 Points considered for determination of the Rayleigh wave velocity

Point	Distance from the Slab Track, m	Distance from the Ballasted Track, m
A	2	1.75
B	4	3.5
C	6	5.25

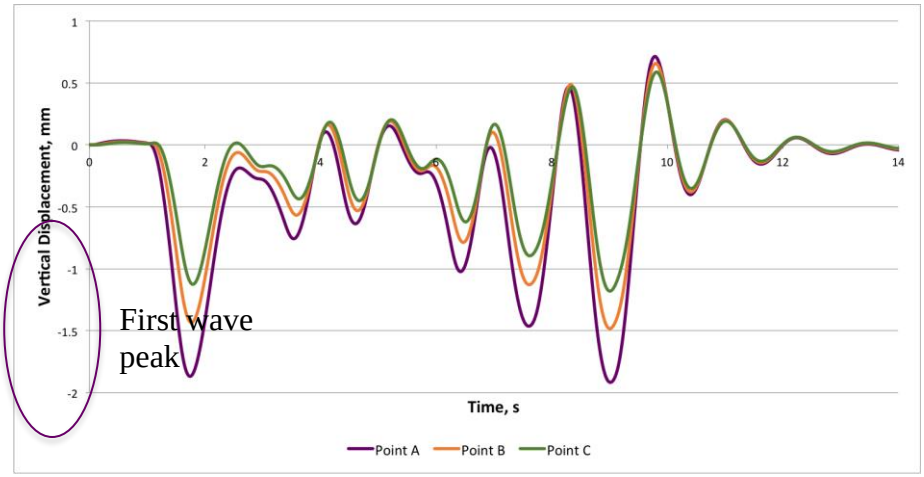

Figure 15 Time dependent vertical displacements at points A, B, C. for the ballasted track (subsoil stiffness, 20MPa)

The first wave peaks are investigated at points A, B, C, and their arrival time is recorded. The distance from the track is plotted against the time of arrival. The slope represents the Rayleigh wave velocity. Figure 16 shows the Rayleigh wave velocity, including the effects of changing train speed, for the ballasted track with subsoil stiffness of 20MPa.

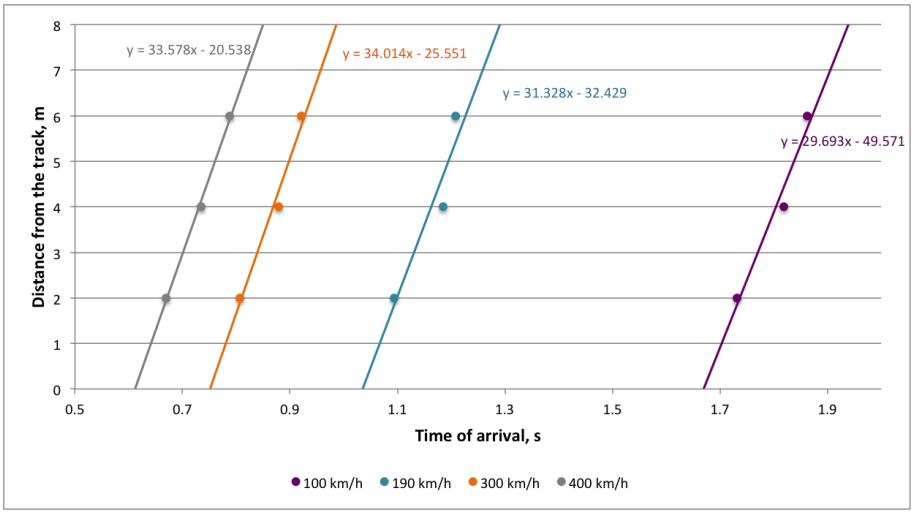

Figure 16 Time of arrival of the first peak vs. the distance from the track for ballasted track on a flat surface (subsoil stiffness 20MPa)

It can be observed that that the Rayleigh wave velocity is independent of the passing train speed. Figure 17 shows the Rayleigh wave velocity values for a train travelling at 300km/h, shown for various subsoil stiffness values.

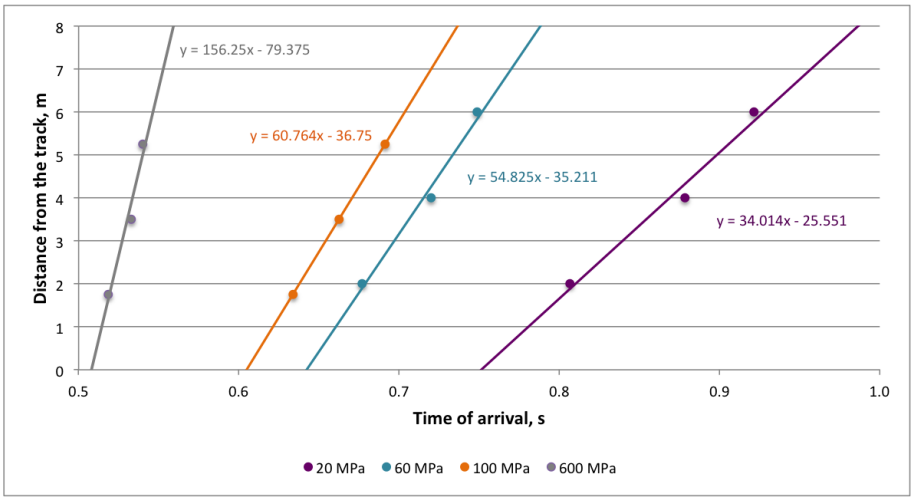

Figure 17 Time of arrival of the first peak vs. the distance from the track for ballasted track on a flat surface for various subsoil stiffness values.

The higher the Rayleigh wave velocity the steeper the slope is, which is in accordance with the theoretical predictions of Rayleigh wave velocity relating to the subsoil stiffness. As the Rayleigh wave velocity shows no variation with different track types, it is further assumed that there is no variation with different track configurations. Mean Rayleigh wave velocity values for different subsoil stiffnesses and track types are summarised in Table 11. The mean Rayleigh wave velocity value is deduced in each case from four lines generated for the following train speeds: 100km/h, 190km/h, 300km/h and 400km/h. A comparison with the theoretical predictions is also added.

Table 11 Mean Rayleigh wave velocity values for different subsoil stiffness values

Subsoil Stiffness, Mpa	Track Type	Mean v_R, km/h	Standard Deviation, %	Fraction of the Theoretical Values
20	Ballasted	110	2.8	0.53
	Slab	116	1.5	0.56
60	Ballasted	183	1.3	0.50
	Slab	189	2.1	0.52
100	Ballasted	238	2.7	0.51
	Slab	238	2.6	0.51
600	Ballasted	563	1.3	0.49
	Slab	563	1.3	0.49

The standard deviation for the Rayleigh velocities does not exceed 3 % of the mean in any one case, again showing that the Rayleigh wave velocity is not affected by the change in either train speed or track type. Discrepancies could have been introduced due to the sampling frequency of the vertical displacement data, in which the time of arrival of the maximum displacement value of the first peak could be slightly shifted. It can, however, be stated that the following relationship holds true for the models developed that $v_R \cong 0.5\ v_{R(theoretical)}$.

The above relationship (experimentally acquired Rayleigh wave velocity values) is used in the analysis, as this shows the Rayleigh wave behaviour of the particular models developed. This could be influenced by material properties, applied loading conditions, derived damping ratios, natural frequency of the particular model, or combination of all.

Table 12 summarises the different subsoil stiffnesses and their corresponding Rayleigh wave velocity values, which will be used in the analysis of the results.

Table 12 Rayleigh wave velocity values used in the further results analyses

Subsoil Stiffness, MPa	20	60	100	600
Rayleigh Wave Velocity, v_R (km/h)	105	182	234	573

MAXIMUM STATIC DISPLACEMENT

The determination of maximum static displacements is of high importance in the analysis, as the values are key to establishing the anticipated relationship – normalised displacement vs normalised train speed. The normalised displacement is calculated dividing the maximum dynamic displacement by the corresponding maximum static displacements.

Maximum static displacement values up to 40m to the right from the track (0m represent the right corner of the track) are shown in Figure 18, Figure 19, Figure 20, and Figure 21 for all four track model configurations (slab/ballasted, flat/embankment).

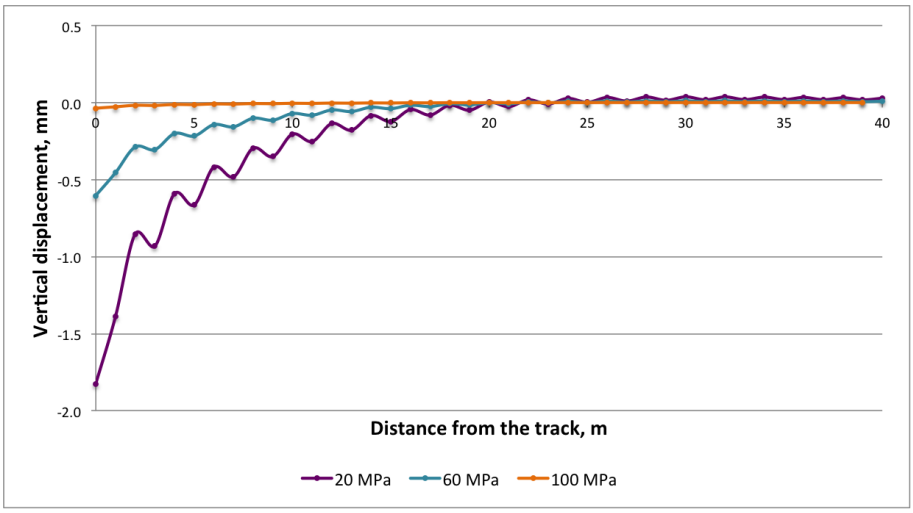

Figure 18 Slab track on flat surface max static displacements for various subsoil stiffness values

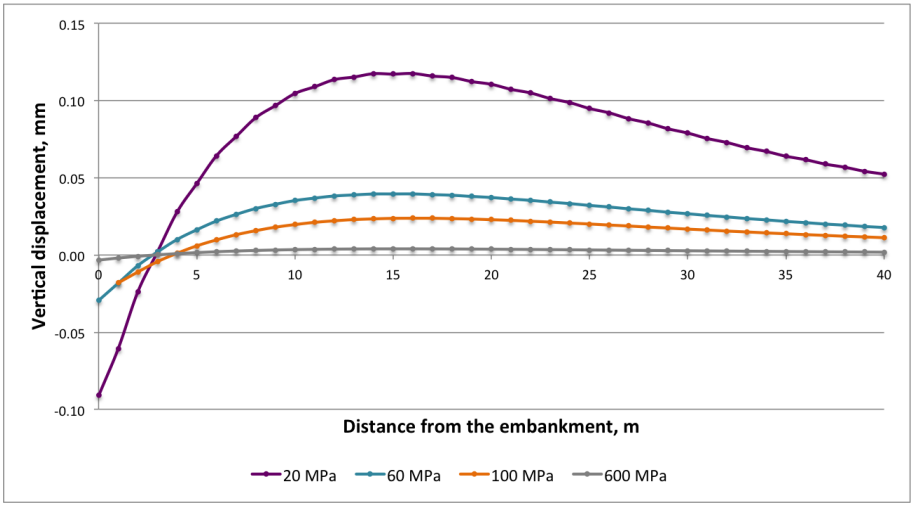

Figure 19 Slab track on embankment max static displacements

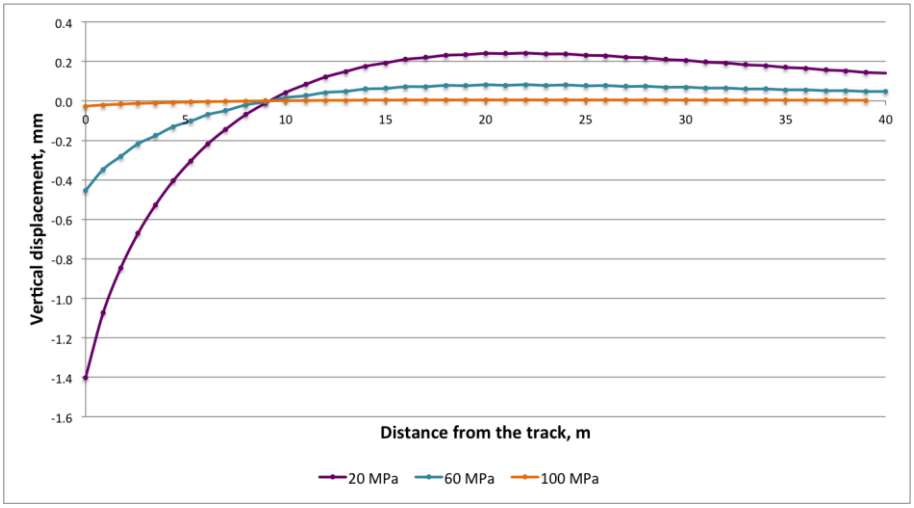

Figure 20 Ballasted track on flat surface max static displacements

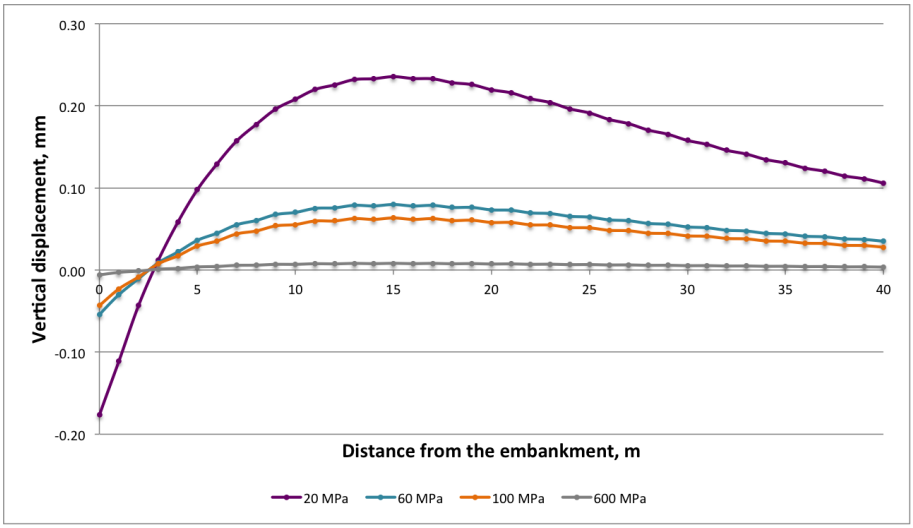

Figure 21 Ballasted track on embankment max static displacements

A substantially higher subsoil stiffness value of 600MPa is included for the embankment model configurations, as the embankment configuration allows for trains to travel at higher speeds and hence a higher Rayleigh wave velocity in the subsoil medium is desired.

MAXIMUM DYNAMIC DISPLACEMENT

The slab track models with the subsoil stiffness of 20MPa were chosen to be the reference models to set a benchmark for comparison with other soil stiffness values under investigation. The maximum dynamic displacement values are acquired from the time domain vertical displacement output data, shown in Figure 22 for the slab track on a flat surface at point C. Normalised maximum dynamic displacement has been plotted against normalised train speed in Figure 23 for the slab track model on a flat surface

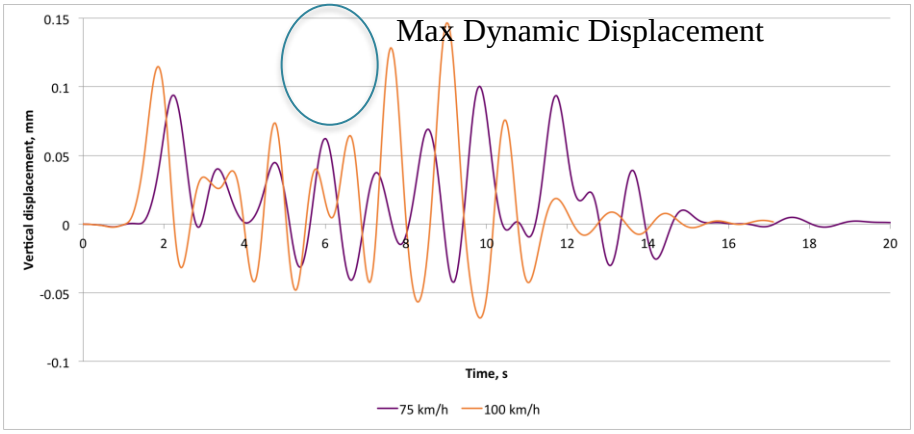

Figure 22 Vertical displacement vs time for slab track on flat surface at point C for different train velocities

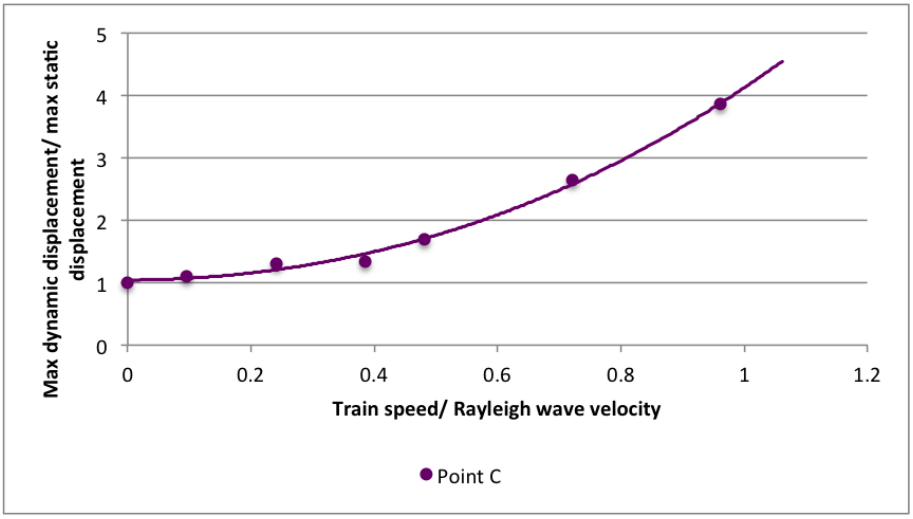

Figure 23 Normalised max dynamic displacement against normalised train speed for the slab track model on a flat surface (subsoil stiffness, 20 MPa)

It can be observed that there is a significant increase in the maximum dynamic displacement values after the train speed has reached half of the Rayleigh wave velocity. The increase from the train travelling at 50km/h to 100km/h is 3.14 times greater for the slab track on a flat surface and 3.86 times greater for the slab track on an embankment than that from 0km/h to 50km/h. Similarly for the ballasted track, the increase from the train travelling at 50 km/h to 100 km/h is 3.32 times greater for the ballasted track on a flat surface and 2.96 times greater for the ballasted track on an embankment than that from 0 km/h to 50 km/h.

The results are summarised in Figure 24 and Figure 25 for all four track model configurations (slab/ballasted, flat/embankment)

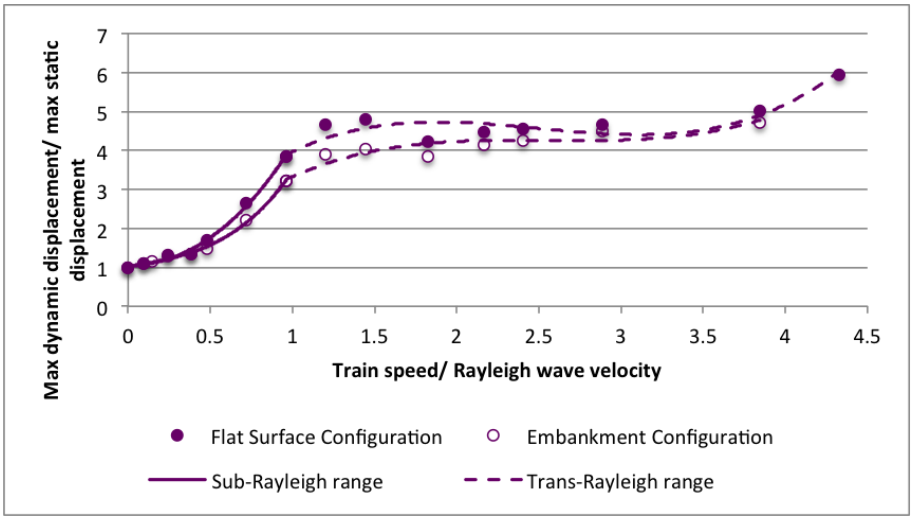

Figure 24 Normalised max dynamic displacement against normalised train speed for slab track model at point A (subsoil stiffness, 20 MPa)

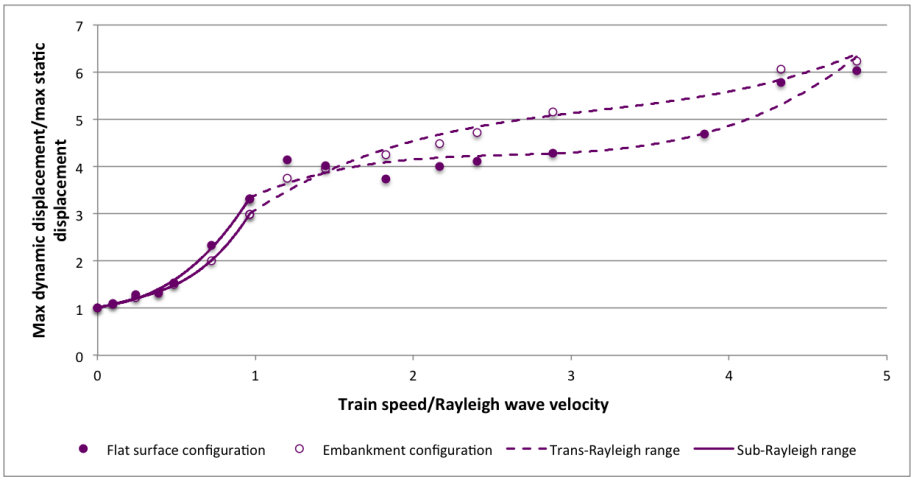

Figure 25 Normalised max dynamic displacement against normalised train speed for ballasted track model at point C (subsoil stiffness, 20 MPa)

It can be seen that there is a behavioural change in the maximum dynamic displacements for different track configurations, as the curve for the slab track on an embankment is less steep than that for the slab track on a flat surface in the sub-Rayleigh range. Additionally, the behaviour of the dynamic displacements significantly changes past the Rayleigh wave velocity. There is no experimental field data to compare the modelling results with; hence, the behavioural change can only be observed. However, according to Krylov et. al (2000), when the train speed lies in the range of $v_R < v < v_{min}$ (where v_R is Rayleigh wave velocity, v is train speed, and v_{min} is track critical velocity), increase in ground vibrations is not as dramatic as for $v = v_R$ when the ground vibration boom is experienced.

PARAMETRIC STUDY

A parametric study was undertaken to investigate the same behaviour for varying subsoil stiffness values. The corresponding normalised curves are shown in Figure 26, Figure 27, Figure 28, and Figure 29 for all four track model configurations (slab/ballasted, flat/embankment). Corresponding field data is also shown (available from three European train lines: Amsterdam-Utrecht, Ledsgard and Stilton Fen, values of which have been replicated from Connolly (2013)). Even though all the previously mentioned train lines run on a ballasted track, the slab track behaviour is investigated and comparability measured.

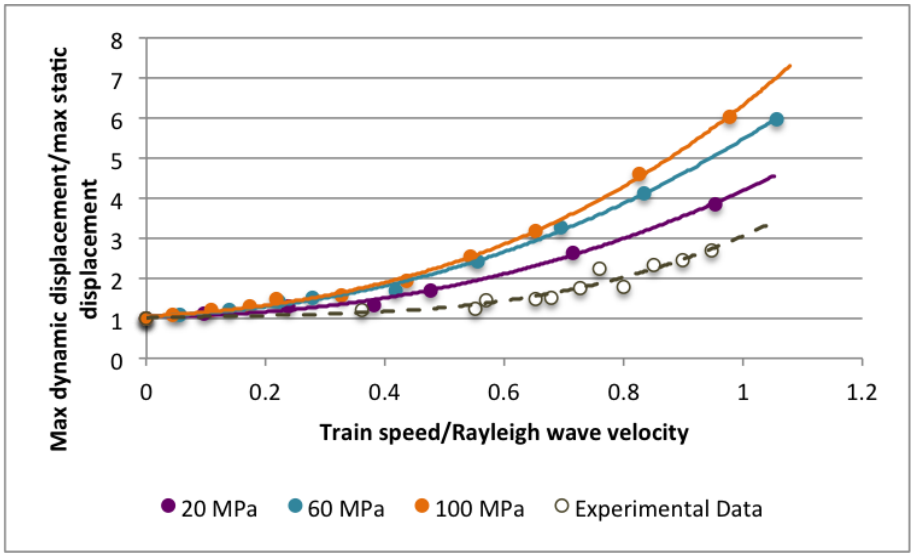

Figure 26 Normalised max dynamic displacement against normalised train speed for slab track model on flat surface at point A

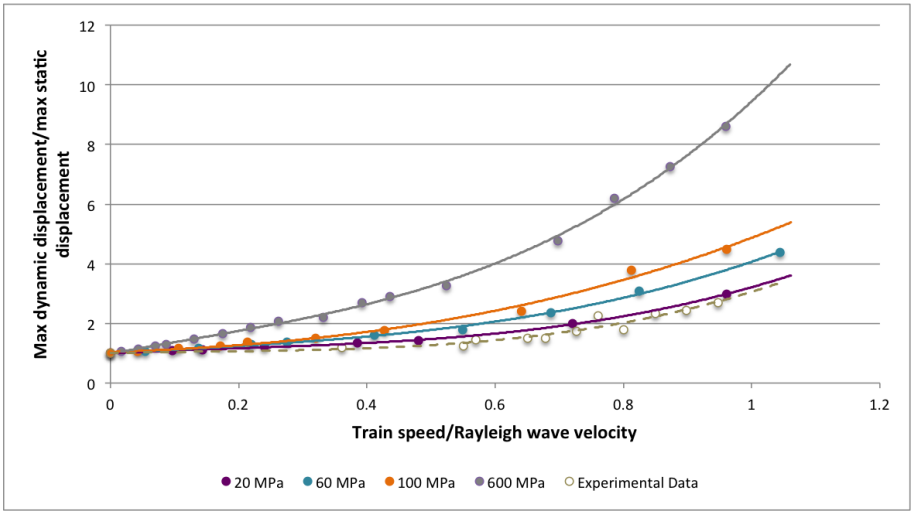

Figure 27 Normalised max dynamic displacement against normalised train speed for slab track model on an embankment at point A

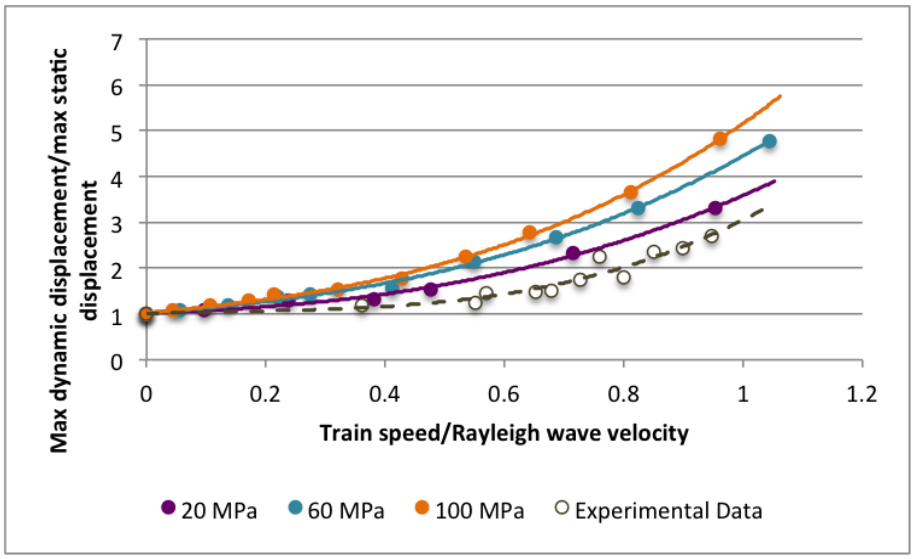

Figure 28 Normalised max dynamic displacement against normalised train speed for ballasted track model on flat surface at point C

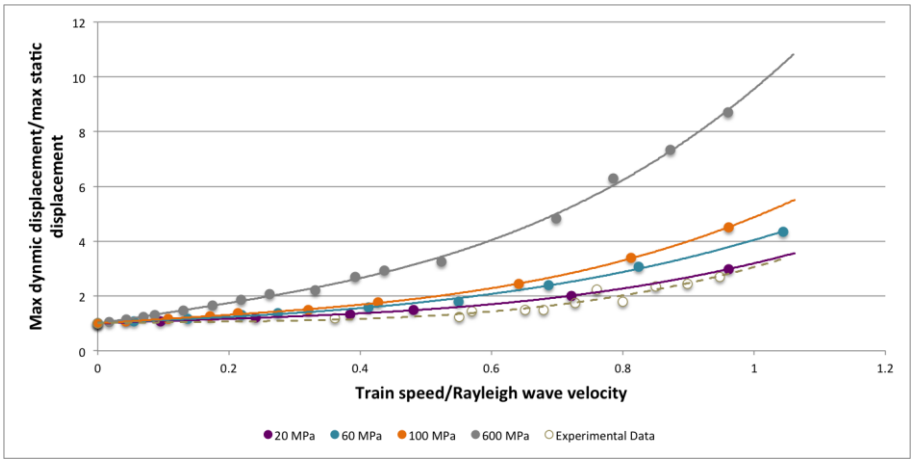

Figure 29 Normalised max dynamic displacement against normalised train speed for ballasted track model on an embankment at point C

It can be observed that the normalised displacement values for the slab track on an embankment are lower than those for the slab track. In other words, the slab track on a flat surface amplifies the vibrations outwards from the track more than the slab track on an embankment.

Comparing with the experimental data, it can be seen that the models have either overestimated the maximum dynamic displacement values or underestimated the maximum static displacement values compared with the field data (or a combination of both). To correlate the model results to the experimental data, the equations for each line were determined to explore a linear scaling for the modelled results. The calculated scaling factors are recorded in Table 13 and Table 14, including the standard deviation values (STD), for all four track model configurations (slab/ballasted, flat/embankment).

Table 13 Linear reduction factors for the normalised max dynamic displacement values and STD for the flat surface model configuration

Subsoil Stiffness, Mpa	Slab Track		Ballasted Track	
	Mean Reduction Factor	STD, %	Mean Reduction Factor	STD, %
20	0.69	2.37	0.8	4.41
60	0.54	2.16	0.65	3.04
100	0.49	2.68	0.59	3.64

Table 14 Linear reduction factors for the normalised max dynamic displacement values and STD for the embankment model configuration

Subsoil Stiffness, Mpa	Slab Track		Ballasted Track	
	Mean Reduction Factor	STD, %	Mean Reduction Factor	STD, %
20	0.9	3.03	0.88	3.88
60	0.72	2.24	0.72	2.57
100	0.6	1.98	0.63	2.53
600	0.34	2.62	0.34	2.56

Application of the scaling factors to the model data produces very tight fit with the experimental data, as can be seen in in the results for the embankment configuration in Figure 30and Figure 31.

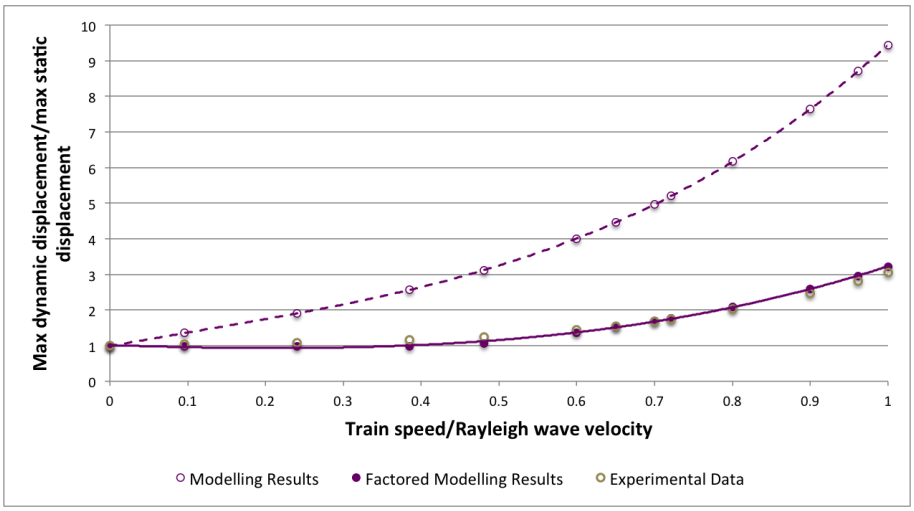

Figure 30 Normalised factored/calibrated and unfactored max dynamic displacement against normalised train speed for the slab track model on an embankment

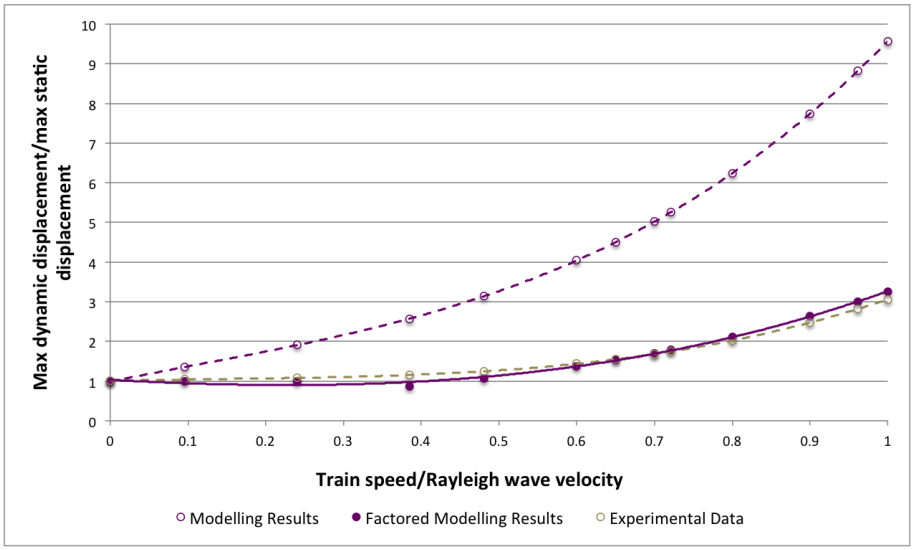

Figure 31 Normalised factored and unfactored max dynamic displacement against normalised train speed for the ballasted track model on an embankment

These results show that the model can successfully replicate the exponential increase in maximum dynamic displacements as a train approaches Rayleigh wave velocity. Furthermore, the model indicates how this behaviour may progress at trans-Rayleigh wave velocity.

It can be concluded that 2-dimensional cross-sectional slab track models can be further explored to facilitate additional track details (simplified in the models) and material properties that would more closely resemble a 'real life' situation (eg, plastic limit, undrained shear strength for the subsoil) as the normalised maximum dynamic displacements increase exponentially after train speed has reached the Rayleigh wave velocity. The same can be observed in the available experimental field data from three European train lines. This significantly reduces the computational costs compared with those for running fully coupled 3-D models to predict the dynamic behaviour from passing train. However, experimental field data should be collected to validate these predictions for slab track.

COMPARISON BETWEEN THE SLAB AND BALLASTED TRACKS

The track models with the subsoil strength of 20 MPa were chosen to represent the key relationships. Normalised displacement has been plotted against normalised train speed in Figure 32 for both the slab and ballasted tracks on a flat surface. As train speed increases, it can be seen that the two curves diverge with the slab track displacement ration increasing more than the ballasted track. However, as can be seen from Figure 33, the absolute values for slab track displacements are significantly smaller than those for the ballasted track and that it can be concluded that the slab track attenuates the vibrations to a higher extent.

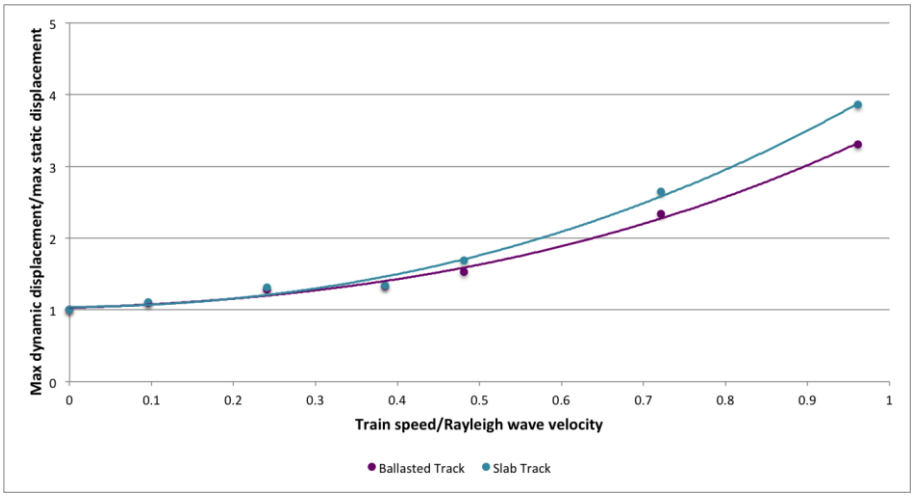

Figure 32 Normalised max dynamic displacement against normalised train speed for ballasted and slab track models on flat surface (subsoil stiffness, 20MPa)

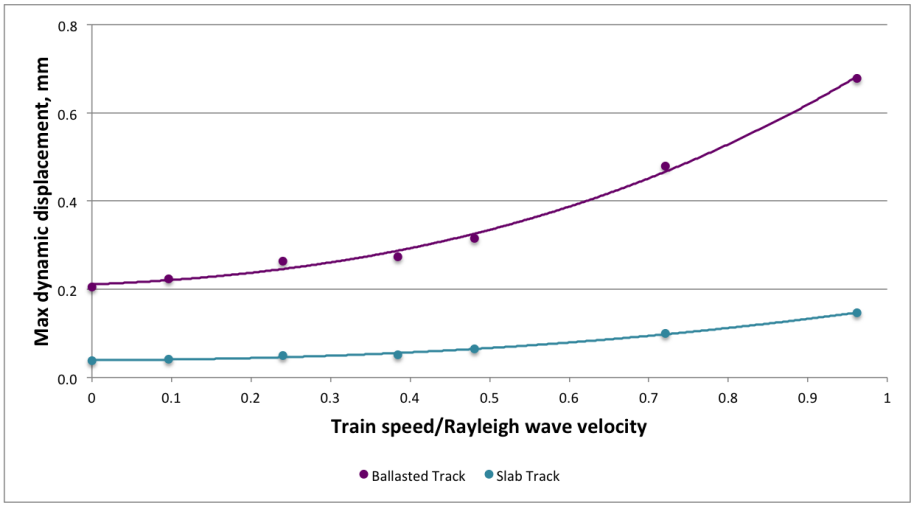

Figure 33 Absolute max dynamic displacement against normalised train speed for ballasted and slab track models on flat surface (subsoil stiffness, 20MPa)

Normalised maximum dynamic displacement has been plotted against normalised train speed in Figure 34 for both the slab track and ballasted track on an embankment. Both curves match suggesting that the Rayleigh wave behaviour does not change for different track types on an embankment. Figure 35 shows the absolute maximum dynamic displacement against the normalised train speed, which are similar to the flat surface results.

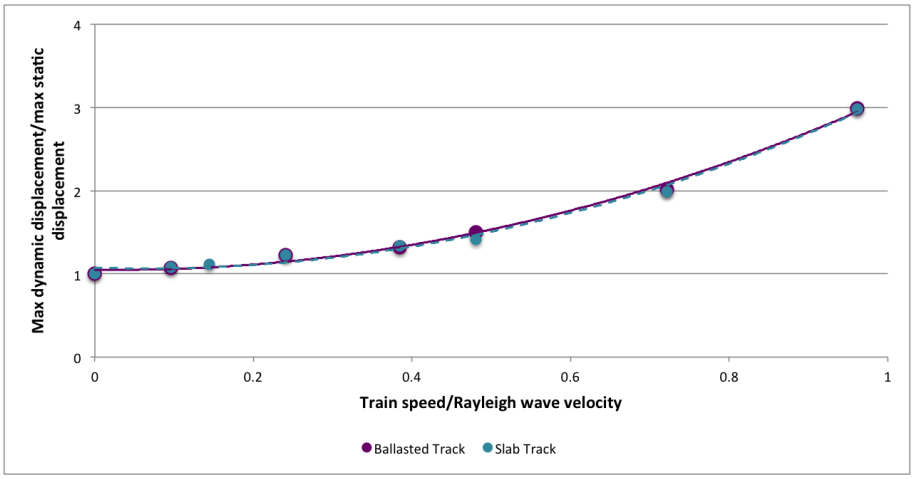

Figure 34 Normalised max dynamic displacement against normalised train speed for ballasted and slab track models on embankment (subsoil stiffness, 20MPa)

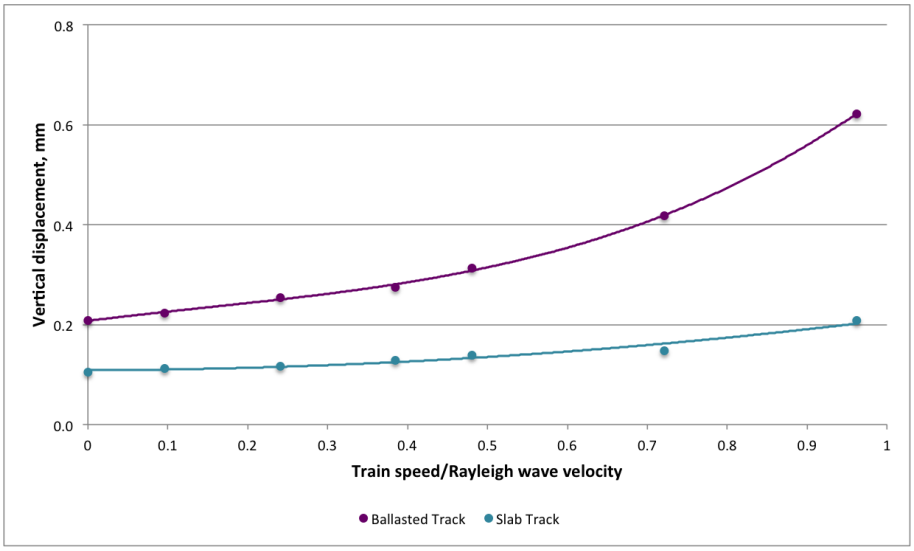

Figure 35 Absolute max dynamic displacement against normalised train speed for ballasted and slab track models on embankment (subsoil strength, 20MPa)

The dynamic behaviour is of greatest interest at $v = 0.7v_R$. The normalised maximum dynamic displacement values for each line were therefore acquired and compared at that point and are shown in Table 15.

Table 15 Max reduction factors of the dynamic displacement for the slab track

Subsoil Stiffness, MPa	20	60	100	600
Max Dynamic Displacement Reduction Factor	0.75	0.70	0.72	0.60

It can be concluded that if a slab track were implemented on the same ground conditions instead of a ballasted track, the vibrations outwards from the track could be reduced by on average 30 %. A final comparison with the experimental data can be seen in Figure 36 (embankment, and subsoil 20MPa).

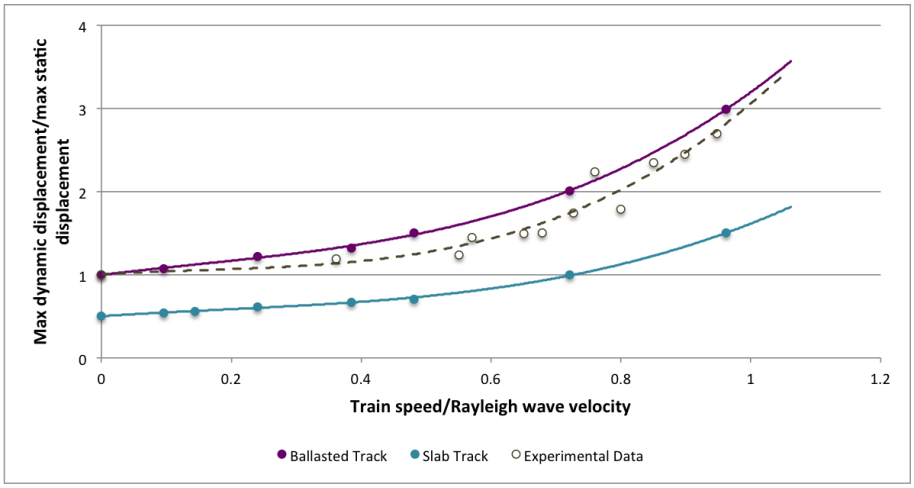

Figure 36 Normalised max dynamic displacement against normalised train speed for ballasted and slab track models on embankment (subsoil stiffness, 20MPa)*

*The concrete slab track prediction is normalised to the ballasted track max static displacement, not its own max static displacement, thus originating at 0.5 on the y-axis rather than 1.

CONCLUSIONS

The study focused on the vertical displacement behaviour on subsoil surface, outwards from either a slab or ballasted track. Dynamic, implicit analysis was performed in Abaqus software in order to explore the behaviour depending on the track type (slab or ballast), track configuration (flat surface or embankment) and varying subsoil stiffness. The aim of the study was to generate normalised displacement vs. normalised train speed curves, and compare them with the experimental field data available from three European train lines: Amsterdam-Utrecht, Ledsgard and Stilton Fen. The scope of the project included changing track type and configuration, as well as loading (train speed) and subsoil stiffness values. Four different final models were developed: slab and ballasted tracks on a flat surface and slab and ballasted tracks on an embankment.

2-D cross-sectional models of a track presented an exponential increase in the maximum dynamic displacement values once the train speed had reached half of the Rayleigh wave velocity. However, the analysis suggests that calibration of the curves are needed to fit the experimental field data, as it appeared that the numerical modelling results have either overestimated the maximum dynamic displacement values or underestimated the maximum static displacement values, or a combination of both. Whilst this can serve as an additional factor of safety for high-speed railway track developments, it might be too conservative (reducing the allowable train speed value, $v = 0.7v_R$) at times leading to inefficiency in the design. This arises due to simplifications in the developed models or, alternatively, due to the limited number of subsoil characterising parameters used: Young's modulus, E, density, ρ, Poisson's ratio, ν, mass proportional damping, α, and stiffness proportional damping, β. In order to avoid these overestimations (an unreliable design), it is of high importance to review the model definitions, as well as the material properties for the models to resemble the real life situation as closely as possible.

After the analysis of the numerical results from the initial model, two main conclusions were drawn:

- Both mass proportional, α, and stiffness proportional, β, damping ratios are of high importance in the dynamic analysis.
- Applied loading frequency and the sampling rate of the output data – both have an effect on the results. The initial model showed behavioural discrepancies between lower and higher train

speeds, i.e., the maximum dynamic displacement values did not increase with elevated train speeds. It was assumed that the wave propagation for the higher speeds (loading period equal to 0.09 s^{-1} for the train travelling at 400 km/h) was restricted by the model definition and interactions of the particular material properties. Hence, the loading frequency was reduced (every 1000^{th} instead of every 10^{th} loading point was used), as well as the sampling frequency was linearly increased with growing train speed. Thus, it allowed the maximum vertical deflections to reach their maximum amplitudes.

After facilitating the conclusions drawn from the numerical analysis of the initial model, two different track types (slab and ballasted) and two different track configurations (flat surface and embankment) were developed for the final models. Several conclusions can be drawn from the analysis:

- Rayleigh wave velocity in the subsoil is independent of both the track type and configuration. It depends on the material properties: Young's modulus, E, density, ρ, and Poisson's ratio, ν. The experimental observations of the arrival time of the first wave peak yielded Rayleigh wave velocity values equal to half of the theoretical predictions, which were further used in the analysis for the result presentation. The explanation could be that, again, the combination of the particular material properties, contact definitions between physical parts, overestimation of one of the damping ratios, or the system's natural frequency could have led to this constant (50%) discrepancy;
- The largest discrepancies between the numerical results and the experimental field data were shown for the slab track on a flat surface where the numerical modelling results showed, on average, a 30% overestimation of the results for the model with subsoil of 20 MPa. However, this is as expected as the field data is related to ballasted track;
- Observations on track configuration: the modelling results for the embankment configuration showed smaller discrepancies with the experimental field data than the results for the flat surface configuration. The results for the slab track on a flat surface showed, on average, an 11% discrepancy with those for the slab track on an embankment (overestimated). Additionally, the results do not differ substantially for the ballasted track on both a flat surface and embankment;
- Observations on track type: Better fit to the experimental data were the numerical modelling results for the ballasted track on both flat surface and embankment, showing, on average, an 11% discrepancy with the experimental results for the models with subsoil of 20 MPa. This can be explained with the fact that the experimental data available are from tracks running on ballast layers.
- Linear scaling can be applied to the numerical results to match the experimental data curve;
- Slab track has a potential to reduce the dynamic vibrations by as much as 30% compared to ballasted track;
- **Main conclusion:** 2-dimensional models can be calibrated to fit the experimental data curve. They can be further explored to facilitate more detailed track geometries and subsoil parameters that would resemble more closely the 'real life' conditions. This, in turn, might lead to significantly reduced computational costs, and a useful tool for industry.

There were many simplifying assumptions throughout this work, including:

- Simplified and very generic track geometries were used in the modelling. Even though it represents the general structure of the track, it does not account for the possible designs. Also, limited geometric range was explored for the physical parts of the track/ embankment/ subsoil system, such as concrete bed, embankment (variety of heights and slopes) etc. To develop a precise calibration system, it is suggested to explore as many track configurations as possible;

- Soil was considered of equal strength and within linear-elastic range throughout the modelling. For example, it did not accommodate the short- term reduction in shear strength. Even though this would increase the complexity of the analysis, these factors must be carefully considered to estimate the degree of relevance in the final numerical results;
- Idealised conditions, such as the track invariability in the longitudinal direction, which allows for the plane strain assumption in the modelling in 2-D, are rarely achieved in practice, thus arguably reducing the applicability of the results. However, additional factors can be sought for the dynamic loading scenarios to account for this;
- Every 1000th loading point was used in the analysis to increase the computational efficiency. While it did resemble a general pattern of the train loading, means should be sought to incorporate the frequency of the raw loading data. Finer mesh and use of the supercomputer would potentially allow the higher loading frequencies to be accordingly analysed.

ACKNOWLEDGEMENTS

The authors gratefully acknowledge the support of their respective universities: The University of Edinburgh, Scotland and The University of Massachusetts, Amherst MA, USA**.**

REFERENCES

AREMA. Manual for Railway Engineering. American Railw Eng & Maint-of-way Assoc 2010.

Britpave, 2016. Why build slab track? [Online] Available at: http://www.britpave.org.uk/RailWhyBuild.ink [Accessed 20 April 2016].

Dieterman, H.A. and Metrikine, V., 1997. Steady-state displacements of a beam on an elastic half-space due to a uniformly moving constant load. *EUROPEAN JOURNAL OF MECHANICS SERIES A SOLIDS*, *16*, pp.295-306.

Cai, C., Zheng, H., Khan, M.S. and Hung, K.C., 2002, April. Modeling of material damping properties in ANSYS. In *CADFEM Users' Meeting & ANSYS Conference* (pp. 9-11).

Connolly, D. P., 2013. Ground borne vibrations from high speed trains (PhD thesis), s.l.: The University of Edinburgh.

Connolly, D. P. & Forde, M. C., 2015. Use of conventional site investigation parameters to calculate critical velocity of trains from Rayleigh waves. *Transportation Research Record*, Volume 2476, pp. 32-36.

Connolly, D. P., Kouroussis, G,. Giannopoulos, A, Verlinden, O, Woodward, P. K. 1 and M. C. Forde, Assessment of railway vibrations using an efficient scoping model, Soil 2 Dyn. Earthq. Eng., 2014, 58 (March): 37-47.

Connolly, D. P., Kouroussis, G,. Laghrouche, O., Ho, C. and M. C. Forde, Benchmarking railway vibrations – Track, vehicle, ground and building effects, *Construction and Building Materials*, Elsevier, Volume 92, 1 September 2015, Pages 64–81, doi: 10.1016/j.conbuildmat.2014.07.042

Esveld, C., 2003. Recent developments in slab track. *European railway review*, 9(2), pp.81-85.

Ferreira, P.A. and Lopez-Pita, A., 2015. Numerical modelling of high speed train/track system for the reduction of vibration levels and maintenance needs of railway tracks. *Construction and Building Materials*, *79*, pp.14-21.

Gao, Y., Huang, H., Ho, C. L., Judge, A. & Chrismer, S., 2015. Field Validation of a Three-dimensional Sandwich Dynamic Track Model. *Submitted for Journal of Sound and Vibration.*

Hall, L., 2003. Simulations and analyses of train-induced ground vibrations in finite element models. *Soil Dynamics and Earthquake Engineering*, *23*(5), pp.403-413.

Huang, H. and Chrismer, S., 2013. Discrete element modeling of ballast settlement under trains moving at "Critical Speeds". *Construction and Building Materials*, *38*, pp.994-1000.

Kaynia, A. M., Madshus, C., 2000. High speed railway lines on soft ground: dynamic behaviour of critical train speed. *Journal of Sound and Vibration*, 231(3), pp. 689-701.

Kaynia, A.M., Madshus, C. and Zackrisson, P., 2000. Ground vibration from high-speed trains: prediction and countermeasure. *Journal of Geotechnical and Geoenvironmental Engineering*, *126*(6), pp.531-537.

Kece E. & Reikalas V., 2016. High speed rail track bed. Evaluating the dynamic response of ballasted track and concrete slab track using numerical analysis (MEng thesis), s.l.: The University of Edinburgh.

Kouroussis, G., Verlinden, O. and Conti, C., 2011. Free field vibrations caused by high-speed lines: measurement and time domain simulation. *Soil Dynamics and Earthquake Engineering*, *31*(4), pp.692-707.

Krylov, V.V., 1995. Generation of ground vibrations by superfast trains. *Applied Acoustics*, *44*(2), pp.149-164.

Krylov, V. V., 2000. High speed lines on soft ground: dynamic soil-track interaction and ground borne vibrations. *Acoustics Bulletin*, 23 (3), pp. 25-26.

Krylov, V. V., Dawson, A. R., Heelis, M. E. & Collop, A. C., 2000. Rail movement and ground waves caused by high-speed trains approaching track-soil critical velocities. *Proceedings of the Institution of Mechanical Engineers, Part F: Journal of Rail and Rapid Transit,* 214(2), pp. 107-116.

Krylov, V. V., 2001. Noise and Vibration from High-Speed Trains. (V. V Krylov, Ed.) (pp. 1–435). Thomas Telford.

Lombaert, G. and Degrande, G., 2009. Ground-borne vibration due to static and dynamic axle loads of InterCity and high-speed trains. *Journal of Sound and Vibration*, *319*(3), pp.1036-1066.

Madshus, C. and Kaynia, A.M., 2000. High-speed railway lines on soft ground: dynamic behaviour at critical train speed. *Journal of Sound and Vibration*, *231*(3), pp.689-701.

Paolucci, R., Maffeis, A., Scandella, L., Stupazzini, M. and Vanini, M., 2003. Numerical prediction of low-frequency ground vibrations induced by high-speed trains at Ledsgaard, Sweden. *Soil Dynamics and Earthquake Engineering*, *23*(6), pp.425-433.

Park, D. and Hashash, Y.M., 2004. Soil damping formulation in nonlinear time domain site response analysis. *Journal of Earthquake Engineering*, *8*(02), pp.249-274.

Powrie, W., Yang, L.A. and Clayton, C.R., 2007. Stress changes in the ground below ballasted railway track during train passage. *Proceedings of the Institution of Mechanical Engineers, Part F: Journal of Rail and Rapid Transit*, *221*(2), pp.247-262.

Rahman, M. and Michelitsch, T., 2006. A note on the formula for the Rayleigh wave speed. *Wave Motion*, *43*(3), pp.272-276.

Rail One, 2011. Rheda 2000 Ballastless Track System. [ONLINE] Available at: http://www.railone.com/fileadmin/daten/05-presse-medien/downloads/broschueren/en/Rheda2000_EN_2011_ebook.pdf. [Accessed 7 November 2016].

Sheng, X., Jones, C.J.C. and Thompson, D.J., 2004. A theoretical model for ground vibration from trains generated by vertical track irregularities. *Journal of sound and vibration*, *272*(3), pp.937-965.

Xia, J., Miller, R.D. and Park, C.B., 1999. Estimation of near-surface shear-wave velocity by inversion of Rayleigh waves. *Geophysics*, *64*(3), pp.691-700.

Yang, L.A., Powrie, W. and Priest, J.A., 2009. Dynamic stress analysis of a ballasted railway track bed during train passage. *Journal of Geotechnical and Geoenvironmental Engineering*, *135*(5), pp.680-689.

Zhai, W., He, Z. and Song, X., 2010. Prediction of high-speed train induced ground vibration based on train-track-ground system model. *Earthquake Engineering and Engineering*